Progress In Electromagnetics Research, PIER 17, 25–43, 1997

HYBRIDIZATION OF SBR AND MoM FOR SCATTERING BY LARGE BODIES WITH INHOMOGENEOUS PROTRUSIONS

F. Ling and J.-M. Jin

Center for Computational Electromagnetics
Department of Electrical and Computer Engineering
University of Illinois at Urbana-Champaign
Urbana, Illinois 61801-2991, USA

1. INTRODUCTION

For analysis of large-scale electromagnetic scattering problems, high-frequency asymptotic methods are fast but approximate, whereas low-frequency numerical methods are accurate but slow. Neither can produce an efficient and accurate solution to scattering by large bodies containing small structures. A promising approach is to combine the best features of both types of methods to produce a hybrid technique that is sufficiently fast, reasonably accurate, and applicable to a class of unsolvable problems such as the scatterers mentioned above. There are two extremes for this type of hybridization. One is simply to superimpose solutions from asymptotic and numerical methods. While this approach is most widely used in practical applications, it neglects the interactions between the two solutions, which can be significant in many problems. The other extreme is to combine an asymptotic and

a numerical method in an exact manner, such as the classical work of combining the method-of-moments (MoM) with the geometrical theory of diffraction (GTD) by Thiele *et al.* [1]–[3]. In this approach, the effect of a large body is included by incorporating its diffraction into the Green's function in the integral equation for the small structures, which accounts for all interactions. The approach is particularly attractive for analyzing the radiation of an antenna placed on a large body, and it has recently been extended to scattering by finned convex objects [4]. While this approach is accurate, it is difficult to implement in a general-purpose computer code because of its complexity.

A more practical approach is to develop a technique that can include all significant interactions and neglect all trivial interactions. A successful example is given in [5] and [6] where the shooting-and-bouncing-ray (SBR) method is combined with the finite-element method (FEM) to solve for the scattering and radiation by a large body with cracks and cavities on its surface. The resulting hybrid technique can produce sufficient accuracy and can be implemented in a general-purpose computer code. In this paper, we employ the same philosophy to develop a technique that combines the SBR method and the MoM to solve for the scattering by large conducting bodies with small structures mounted on their surfaces. We note that since the nature of this problem is different from that in [5], the formulation is also different.

To be more specific, in the proposed technique, an integral equation is first derived for the currents in the entire object, including the large body and the small structure. By choosing a proper Green's function that satisfies certain boundary conditions on the surface of the large body, the integral equation is reduced to an integral equation over the surface or volume of the small structure, depending on its material composition. Application of the MoM to this equation with an approximate Green's function yields an admittance matrix, which characterizes the small structure. When multiplied by the incident field on the small structure, which is calculated using the SBR method, the admittance matrix yields the currents on the small structure, which radiate in the presence of the large body. The radiated field from these currents, or the scattered field contributed by the small structure, is then calculated using the SBR method with the aid of the reciprocity theorem.

For most problems, the formulation described above can yield a satisfactory solution. However, for some problems, an approximate

Green's function can be difficult to obtain and the resultant solution can be rather inaccurate. In this case, the accuracy of the approximate solution can be improved using an iterative approach, similar to the methods employed in [7]–[9]. This iterative approach can also be applied to the case of multiple small structures having mutual interactions. As a result, although the hybrid technique presented is approximate, its accuracy can be improved systematically when necessary. In this paper, we implement this technique for two-dimensional scattering to evaluate its accuracy, efficiency, and capability.

2. FORMULATION

Consider the problem of wave scattering by a large, perfectly conducting body with a small protruding structure, whose cross-section is illustrated in Fig. 1. The protruding structure can be a perfect conductor or a dielectric/magnetic material or any combination of these. For transverse magnetic (TM) incidence, the electric field E_z satisfies the wave equation

$$\nabla \cdot \left[\frac{1}{\mu_r(\boldsymbol{\rho})} \nabla E_z(\boldsymbol{\rho}) \right] + k_0^2 \epsilon_r(\boldsymbol{\rho}) E_z(\boldsymbol{\rho}) = j\omega\mu_0 J_z(\boldsymbol{\rho}) \tag{1}$$

where k_0 is the free-space wavenumber, (ϵ_r, μ_r) are the relative permittivity and permeability, respectively, and J_z is the source.

To formulate an integral equation for E_z, we multiply (1) with a Green's function $G_E(\boldsymbol{\rho}, \boldsymbol{\rho}')$, which satisfies

$$\nabla^2 G_E(\boldsymbol{\rho}, \boldsymbol{\rho}') + k_0^2 G_E(\boldsymbol{\rho}) = -\delta(\boldsymbol{\rho} - \boldsymbol{\rho}') \tag{2}$$

and integrate over the entire region. Following the procedure described in [10], we obtain

$$\begin{aligned} \frac{1}{\mu_r(\boldsymbol{\rho})} E_z(\boldsymbol{\rho}) = E_z^{inc}(\boldsymbol{\rho}) &+ k_0^2 \iint_\Omega \left[\epsilon_r(\boldsymbol{\rho}') - \frac{1}{\mu_r(\boldsymbol{\rho}')} \right] E_z(\boldsymbol{\rho}') G_E(\boldsymbol{\rho}, \boldsymbol{\rho}') ds' \\ &+ \iint_\Omega \nabla' \left[\frac{1}{\mu_r(\boldsymbol{\rho}')} \right] \cdot \left[E_z(\boldsymbol{\rho}') \nabla' G_E(\boldsymbol{\rho}, \boldsymbol{\rho}') \right] ds' \\ &+ \int_{\Gamma_d} \left[\frac{1}{\mu_r(\boldsymbol{\rho}'_+)} - \frac{1}{\mu_r(\boldsymbol{\rho}'_-)} \right] E_z(\boldsymbol{\rho}') \frac{\partial G_E(\boldsymbol{\rho}, \boldsymbol{\rho}')}{\partial n'_d} dl' \\ &- j\omega\mu_0 \int_{\Gamma_c} J_z(\boldsymbol{\rho}') G_E(\boldsymbol{\rho}, \boldsymbol{\rho}') dl' \end{aligned} \tag{3}$$

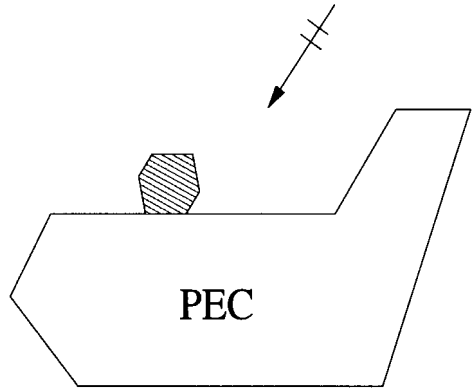

Figure 1. Original problem: A large PEC body with a small protrusion.

where Ω denotes the dielectric region, Γ_d denotes the interface where μ_r changes abruptly, and Γ_c denotes the conducting surface. The normal unit vector points from the "–" side to the "+" side on Γ_d and outward on Γ_c. The incident field $E_z^{inc}(\boldsymbol{\rho})$ is given by

$$E_z^{inc}(\boldsymbol{\rho}) = -j\omega\mu_0 \iint_{\Omega_s} J_z(\boldsymbol{\rho}')G_E(\boldsymbol{\rho},\boldsymbol{\rho}')ds' \tag{4}$$

where Ω_s denotes the source region.

Since Γ_c includes the entire surface of the conductor, a numerical solution of (3) requires the discretization of the entire scatterer. However, if we choose the Green's function to satisfy the boundary condition

$$G_E(\boldsymbol{\rho},\boldsymbol{\rho}') = 0 \qquad \boldsymbol{\rho} \text{ on } \Gamma_b \tag{5}$$

where Γ_b is the surface of the scatterer without the protruding structure (see Fig. 2), the integral on the surface of the large object disappears, and (3) becomes

$$\frac{1}{\mu_r(\boldsymbol{\rho})}E_z(\boldsymbol{\rho}) = E_z^{inc}(\boldsymbol{\rho}) + k_0^2 \iint_{\Omega} \left[\epsilon_r(\boldsymbol{\rho}') - \frac{1}{\mu_r(\boldsymbol{\rho}')}\right] E_z(\boldsymbol{\rho}')G_E(\boldsymbol{\rho},\boldsymbol{\rho}')ds'$$
$$+ \iint_{\Omega} \nabla' \left[\frac{1}{\mu_r(\boldsymbol{\rho}')}\right] \cdot \left[E_z(\boldsymbol{\rho}')\nabla' G_E(\boldsymbol{\rho},\boldsymbol{\rho}')\right] ds'$$

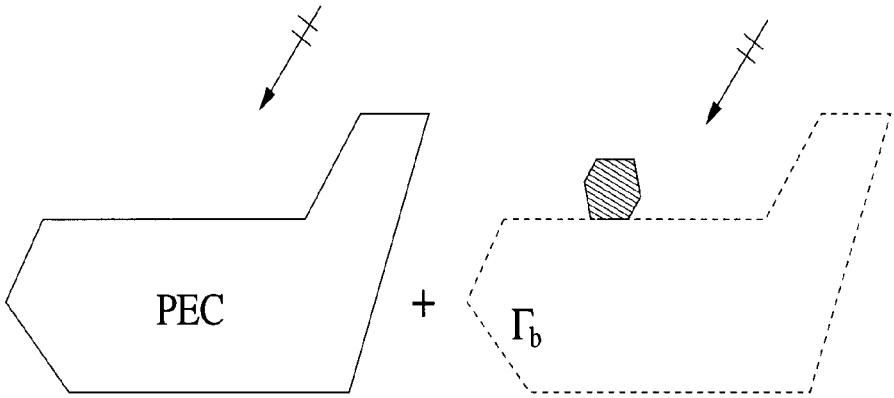

Figure 2. Equivalent problems: One for high-frequency method and the other for numerical method.

$$+\int_{\Gamma_d}\left[\frac{1}{\mu_r(\boldsymbol{\rho}'_+)}-\frac{1}{\mu_r(\boldsymbol{\rho}'_-)}\right]E_z(\boldsymbol{\rho}')\frac{\partial G_E(\boldsymbol{\rho},\boldsymbol{\rho}')}{\partial n'_d}dl'$$
$$-j\omega\mu_0\int_{\Gamma'_c}J_z(\boldsymbol{\rho}')G_E(\boldsymbol{\rho},\boldsymbol{\rho}')dl' \tag{6}$$

where Γ'_c denotes the conducting surface of the protruding structure. Note that when (5) is used, the incident field E_z^{inc} is the field radiated by J_z in the presence of the large body.

Equation (6) can be solved using the MoM described in [11] provided that we know the expression of $G_E(\boldsymbol{\rho},\boldsymbol{\rho}')$. The discretization will be limited to the dielectric region and the surface of the conductor in the protrusion. If the protrusion is on a locally flat surface, $G_E(\boldsymbol{\rho},\boldsymbol{\rho}')$ can be written into two parts

$$G_E(\boldsymbol{\rho},\boldsymbol{\rho}')=G_{Ehalf}(\boldsymbol{\rho},\boldsymbol{\rho}')+G_{Ediff}(\boldsymbol{\rho},\boldsymbol{\rho}') \tag{7}$$

where the first part corresponds to that for a half-space, and the second part is due to the diffraction and reflection seen by the protrusion. Whereas the expression for $G_{Ehalf}(\boldsymbol{\rho},\boldsymbol{\rho}')$ is readily available, the expression for $G_{Ediff}(\boldsymbol{\rho},\boldsymbol{\rho}')$ is often difficult, if not impossible, to obtain. Although the effect of $G_{Ediff}(\boldsymbol{\rho},\boldsymbol{\rho}')$ can still be included in the MoM solution, as was done in [1]–[4], its numerical implementation is complicated and dependent on the geometry of the large object. To simplify

the MoM solution and effectively decouple the MoM and SBR computations, we neglect $G_{Ediff}(\boldsymbol{\rho}, \boldsymbol{\rho}')$ in the MoM solution of (6), and, doing so, we neglect the field scattered by the protrusion, diffracted and/or reflected back to the protrusion by the large object, and scattered by the protrusion again. In most cases, this field is unimportant. However, when necessary it can be recovered by using an iterative approach discussed later.

The MoM discretization of (6) is straightforward, and it results in a matrix equation

$$[Z] \begin{Bmatrix} E_\Omega \\ E_d \\ J_c \end{Bmatrix} = \left\{ E^{inc} \right\} \tag{8}$$

where E_Ω and E_d denote the discretized fields in Ω and on Γ_d, respectively, J_c denotes the current on the conducting surface of the protrusion, and E^{inc} denotes the incident field on the protrusion in the presence of the large object. The incident field can be calculated effectively using the SBR method [12]–[14].

Because of the simplification of $G_E(\boldsymbol{\rho}, \boldsymbol{\rho}')$, the calculation of $[Z]$ is independent of the geometry of the large body. Thus, $[Z]$ can be computed and inverted beforehand. Once this is done, the field and current in the protrusion can be obtained by

$$\begin{Bmatrix} E_\Omega \\ E_d \\ J_c \end{Bmatrix} = [Z]^{-1} \left\{ E^{inc} \right\}. \tag{9}$$

Once the fields and currents are computed, we then have to evaluate the scattered field in the far zone. Theoretically, we can employ (6) to calculate this field. However, the expression for $G_E(\boldsymbol{\rho}, \boldsymbol{\rho}')$ is usually unknown and replacing it by $G_{Ehalf}(\boldsymbol{\rho}, \boldsymbol{\rho}')$ here would neglect the field scattered by the protrusion and diffracted and/or reflected to the observation point, resulting in an error whose magnitude is comparable to the field scattered directly to the observation point. There are two approaches to alleviate this problem. One approach is to first compute the field scattered by the protrusion over a small half circle enclosing the protrusion. This field is then converted into many rays which shoot along the radial directions. Each ray is traced as it bounces

around the large object and the bounces are governed by geometrical optics (GO). At the last hit point, or at each and every hit point, a physical-optics (PO) type integration is performed to determine the ray contribution to the scattered field. The final result is the summation of the contribution from all the rays. This approach has the advantage of simultaneously computing the scattered field in all directions. However, to obtain accurate results, the field on the half circle enclosing the protrusion must be divided into many rays and to trace each ray, its divergence factor must be calculated and tracked. Moreover, the process has to be repeated for each element in the protrusion.

In this work, we use a second approach which employs reciprocity theorem. In this approach, we place an infinitely long current filament at the observation point. The electric field radiated by this current satisfies the equation

$$\nabla^2 E_z'(\boldsymbol{\rho}) + k_0^2 E_z'(\boldsymbol{\rho}) = j\omega\mu_0 J_0 \delta(\boldsymbol{\rho} - \boldsymbol{\rho}_o) \tag{10}$$

where $\boldsymbol{\rho}_o$ denotes the observation point. This equation has a well-known solution given by

$$E_z'(\boldsymbol{\rho}) = -\frac{\omega\mu_0 J_0}{4} H_0^{(2)}(k_0 \left|\boldsymbol{\rho} - \boldsymbol{\rho}_o\right|). \tag{11}$$

If $\boldsymbol{\rho}_o$ is far away from $\boldsymbol{\rho}$ and $\boldsymbol{\rho}$ is near the origin of the chosen coordinates, $E_z'(\boldsymbol{\rho})$ becomes

$$E_z'(\boldsymbol{\rho}) = -\eta_0 J_0 \sqrt{\frac{jk_0}{8\pi\rho_o}} e^{-jk_0\rho_o} e^{jk_0(x\cos\theta + y\sin\theta)} \tag{12}$$

where η_0 is the free-space intrinsic impedance. Apparently, if we choose

$$J_0 = -\frac{1}{\eta_0}\sqrt{\frac{8\pi\rho_o}{jk_0}} e^{jk_0\rho_o} \tag{13}$$

$E_z'(\boldsymbol{\rho})$ then becomes

$$E_z'(\boldsymbol{\rho}) = e^{jk_0(x\cos\theta + y\sin\theta)} \tag{14}$$

which is recognized as a plane wave incident from the direction of the observation point. If the current filament is placed at the observation point in the presence of the large object without the protrusion, the

resulting fields can be calculated conveniently using either PO or the SBR method. Denoting these fields as $\mathbf{E}^{sbr}$ and $\mathbf{H}^{sbr}$, multiplying E_z^{sbr} with (1), and integrating over the entire region yields

$$\begin{aligned} E_z(\boldsymbol{\rho}_o) = & \\ & E_z^{sbr}(\boldsymbol{\rho}_o) - \frac{1}{j\omega\mu_0 J_0}\Bigg\{ k_0^2 \iint_\Omega \left[\epsilon_r(\boldsymbol{\rho}') - \frac{1}{\mu_r(\boldsymbol{\rho}')}\right] E_z(\boldsymbol{\rho}') E_z^{sbr}(\boldsymbol{\rho}') ds' \\ & + j\omega\mu_0 \iint_\Omega \left[\hat{z} \times \nabla' \frac{1}{\mu_r(\boldsymbol{\rho}')}\right] \cdot \left[E_z(\boldsymbol{\rho}') \mathbf{H}^{sbr}(\boldsymbol{\rho}')\right] ds' \\ & - j\omega\mu_0 \int_{\Gamma_d} \left[\frac{1}{\mu_r(\boldsymbol{\rho}'_+)} - \frac{1}{\mu_r(\boldsymbol{\rho}'_-)}\right] E_z(\boldsymbol{\rho}') H_t^{sbr}(\boldsymbol{\rho}') dl' \\ & - j\omega\mu_0 \int_{\Gamma'_c} J_z(\boldsymbol{\rho}') E_z^{sbr}(\boldsymbol{\rho}') dl' \Bigg\} \end{aligned} \tag{15}$$

which is similar to (6). Since E_z and J_z have already been computed, the integrals in (15) can be readily evaluated. In particular, if the monostatic radar cross section (RCS) is of interest, E_z^{sbr} is the same as E_z^{inc} in (6).

For the transverse electric (TE) incidence, the derivation is similar. The integral equation corresponding to (6) becomes

$$\begin{aligned} \frac{1}{\epsilon_r(\boldsymbol{\rho})} H_z(\boldsymbol{\rho}) = & H_z^{inc}(\boldsymbol{\rho}) + k_0^2 \iint_\Omega \left[\mu_r(\boldsymbol{\rho}') - \frac{1}{\epsilon_r(\boldsymbol{\rho}')}\right] H_z(\boldsymbol{\rho}') G_H(\boldsymbol{\rho}, \boldsymbol{\rho}') ds' \\ & + \iint_\Omega \nabla' \left[\frac{1}{\epsilon_r(\boldsymbol{\rho}')}\right] \cdot \left[H_z(\boldsymbol{\rho}') \nabla' G_H(\boldsymbol{\rho}, \boldsymbol{\rho}')\right] ds' \\ & + \int_{\Gamma_d} \left[\frac{1}{\epsilon_r(\boldsymbol{\rho}'_+)} - \frac{1}{\epsilon_r(\boldsymbol{\rho}'_-)}\right] H_z(\boldsymbol{\rho}') \frac{\partial G_H(\boldsymbol{\rho}, \boldsymbol{\rho}')}{\partial n_{d'}} dl' \\ & + \int_{\Gamma'_c} J_t(\boldsymbol{\rho}') \frac{\partial G_H(\boldsymbol{\rho}, \boldsymbol{\rho}')}{\partial n'_c} dl' \end{aligned} \tag{16}$$

and the expression for the far field is

$$\begin{aligned} H_z(\boldsymbol{\rho}_o) = & \\ & H_z^{sbr}(\boldsymbol{\rho}_o) - \frac{1}{j\omega\epsilon_0 M_0}\Bigg\{ k_0^2 \iint_\Omega \left[\mu_r(\boldsymbol{\rho}') - \frac{1}{\epsilon_r(\boldsymbol{\rho}')}\right] H_z(\boldsymbol{\rho}') H_z^{sbr}(\boldsymbol{\rho}') ds' \\ & - j\omega\epsilon_0 \iint_\Omega \left[\hat{z} \times \nabla' \frac{1}{\epsilon_r(\boldsymbol{\rho}')}\right] \cdot \left[H_z(\boldsymbol{\rho}') \mathbf{E}^{sbr}(\boldsymbol{\rho}')\right] ds' \end{aligned}$$

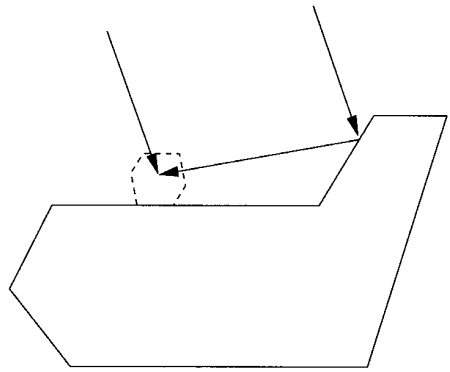

Figure 3. Effects included in the formulation: Direct and indirect incident fields and, by reciprocity, direct and indirect scattered fields.

$$+ j\omega\epsilon_0 \int_{\Gamma_d} \left[\frac{1}{\epsilon_r(\boldsymbol{\rho}'_+)} - \frac{1}{\epsilon_r(\boldsymbol{\rho}'_-)} \right] H_z(\boldsymbol{\rho}') E_t^{sbr}(\boldsymbol{\rho}') dl'$$
$$+ j\omega\epsilon_0 \int_{\Gamma'_c} J_t(\boldsymbol{\rho}') E_t^{sbr}(\boldsymbol{\rho}') dl' \Bigg\} \tag{17}$$

where M_0 is given by

$$M_0 = -\eta_0 \sqrt{\frac{8\pi\rho_o}{jk_0}} e^{jk_0\rho_o}. \tag{18}$$

3. ITERATVE IMPROVEMENT

Because of the use of the SBR method, E_z^{inc} in (6) and H_z^{inc} in (16) include not only the direct incident field, but also the fields reflected and multiply-bounced by the large body, as shown in Fig. 3. Generally speaking, the magnitude of the indirect incident field is comparable to that of the direct field, so neglecting either of them will result in a significant error in the calculation of E_z^{inc} and H_z^{inc}. Similarly, since E_z^{sbr} in (15) and H_z^{sbr} in (17) are calculated using the SBR method, the reflection and multiple bounces are also included in the scattered-field calculation. Therefore, all major interactions between the SBR and MoM have been included.

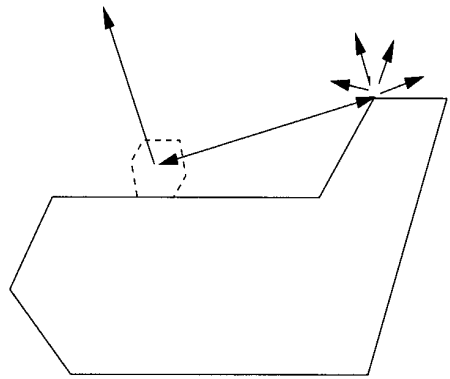

Figure 4. Effects not included in the formulation: Field scattered by the protrusion, diffracted and/or reflected back to the protrusion by the large object, and scattered by the protrusion again. These effects can be recovered using an iterative approach when necessary.

The only approximation in the hybrid technique is introduced by the approximate Green's function, formed by neglecting the second term in (7). As pointed out earlier, this neglects the field scattered by the protrusion, reflected and/or diffracted back to the protrusion by the large object, and scattered by the protrusion again, as illustrated in Fig. 4. In most problems, this contribution is insignificant. However, when the protrusion is very close to edges and reflecting surfaces, the contribution can become significant and its omission can cause a substantial error in the solution. Here, we describe an iterative approach, similar to those in [7]–[9], to reduce the error systematically.

In this iterative approach, we use the current on the protrusion obtained from (9) as the initial value and then calculate the field produced by this current in the presence of the large body. This field can be considered as the secondary incident field, which, when superimposed to the E_z^{inc} and H_z^{inc}, yields a new incident field on the protrusion. Using this as the incident field in (9), we obtain a new, improved current on the protrusion. This process is repeated N times until a stable value for the current is reached. The process can be expressed as

$$\{J_n\} = [Z]^{-1}\left\{E^{inc} + E(\{J_{n-1}\})\right\} \tag{19}$$

where n denotes the number of iteration, $E(\{J_{n-1}\})$ denotes the field

on the protrusion produced by the current J_{n-1} on the protrusion, which can be calculated using either PO or the SBR method.

A similar approach can be employed for large bodies with multiple protrusions. When each protrusion is characterized using the MoM, the interaction between them is neglected. To recover this interaction, we can first analyze protrusions separately and obtain the current on each protrusion. We then choose the current on one of the protrusions as the excitation to obtain the secondary incident fields on other protrusions, which then yield new currents. This process can be repeated until the convergence is reached. For the case with two protrusions, the process can be expressed as

$$\{J_{1,n}\} = [Z_1]^{-1} \left\{ E_1^{inc} + E_1(\{J_{2,n-1}\}) \right\} \tag{20}$$

$$\{J_{2,n}\} = [Z_2]^{-1} \left\{ E_2^{inc} + E_2(\{J_{1,n-1}\}) \right\} \tag{21}$$

$E_i(\{J_{j,n-1}\})$ denotes the field on the i th protrusion produced by the current on the j th protrusion, which can again be calculated using either PO or the SBR method.

4. NUMERICAL RESULTS

To demonstrate the accuracy of the proposed hybrid technique, we present some examples, in which the incident wave is assumed to be a plane wave and the pulse basis functions and point matching are used for the MoM computations.

The first example is a small conducting protrusion at the center of the surface of a large perfectly electric-conducting (PEC) cylinder. The monostatic radar echo width (REW) for the TM and TE cases is shown in Fig. 5. As can be seen, the results by the hybrid technique are in good agreement with those computed by the MoM alone. In this case, the contribution of G_{diff} is much smaller than that of G_{half}, and its omission does not introduce a noticeable error in the scattered-field computation. Therefore, no iteration is necessary. Also presented are the results without the protrusion to demonstrate the significance of the small protrusion.

To show the capability of handling inhomogeneous protrusions, the scatterer in Fig. 5 is reconsidered and this time the protrusion is coated with a layer of material having the relative permittivity $\epsilon_r = 2.5 - j1.0$, the relative permeability $\mu_r = 1.5 - j1.0$, and thickness $t = 0.2\lambda$. The

results are shown in Fig. 6. Again, good agreement is observed between the hybrid and MoM solutions, and no iteration is necessary.

The next two examples show the effectiveness of the iterative approach. The first has two protrusions closely spaced on a large PEC cylinder. First, we analyze the two protrusions independently and, hence, no interaction between them is included. As can be seen in Fig. 7, the results have a significant error when the incident angle is less than 35 degrees. This error is, however, reduced significantly when the iterative approach is applied with 8 iterations.

The second example is an L-shaped conducting body with a protrusion on the surface. This problem differs from the former ones in that both incident and scattered fields can have multiple bounces. First, we neglect the contribution of G_{diff}, and the results obtained are given in Fig. 8 where a noticeable error is observed. This is expected because the protrusion is close to the reflecting surface. The results obtained using the iterative approach with 10 iterations are shown in Fig. 9, which demonstrates clearly that the iterative approach is an effective method to improve the accuracy for such a problem. Finally, we note that the L-shape is chosen here because it represents the worst configuration. If the wall parallel to the protrusion is slanted, the initial solution would have better accuracy and the iteration would converge even more quickly.

To illustrate the efficiency of the hybrid method, let us first examine its complexity as compared to that of the MoM. Assume that the largest dimension of the large body is L and the largest dimension of the small protrusion is l. The MoM solution would require operational count proportional to L^3 and memory proportional to L^2. The hybrid solution without iteration would require operational count proportional to l^3+L and memory proportional to l^2. The hybrid solution with iteration would then require operational count proportional to l^3+l^2L and memory proportional to l^2. As a result, the computing time, compared to that of the MoM, is reduced to $(l^3+L)/L^3$ for the hybrid solution without iteration and $(l^3+l^2L)/L^3$ with iteration. The memory requirement is reduced to $(l/L)^2$ of that for the MoM. For example, the MoM solution in Fig. 5 has 2560 unknowns and takes 1714.4 seconds on a workstation whereas the SBR/MoM solution has 200 unknowns and takes only 3.4 seconds on the same workstation for all incidence angles. The MoM solution in Figs. 8 and 9 has 3520 unknowns and takes 4071.8 seconds whereas the SBR/MoM solution has

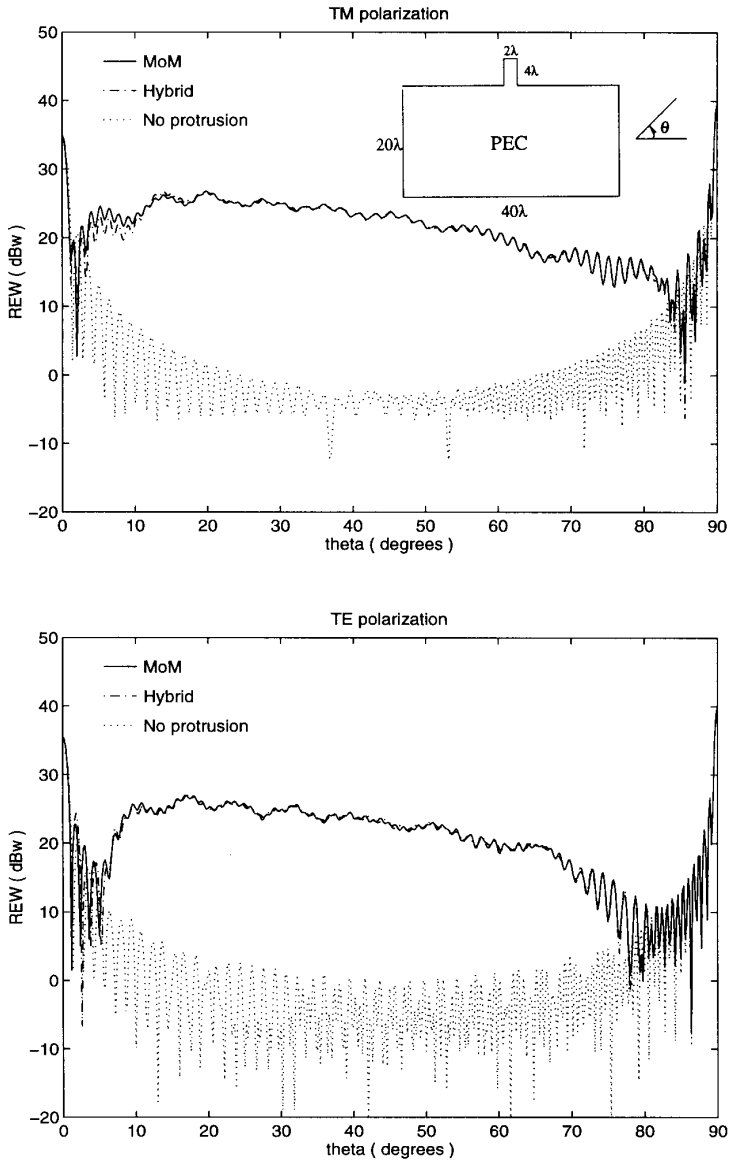

Figure 5. Comparison of the monostatic echo-width calculated by the hybrid SBR/MoM and the MoM for a body with a conducting protrusion.

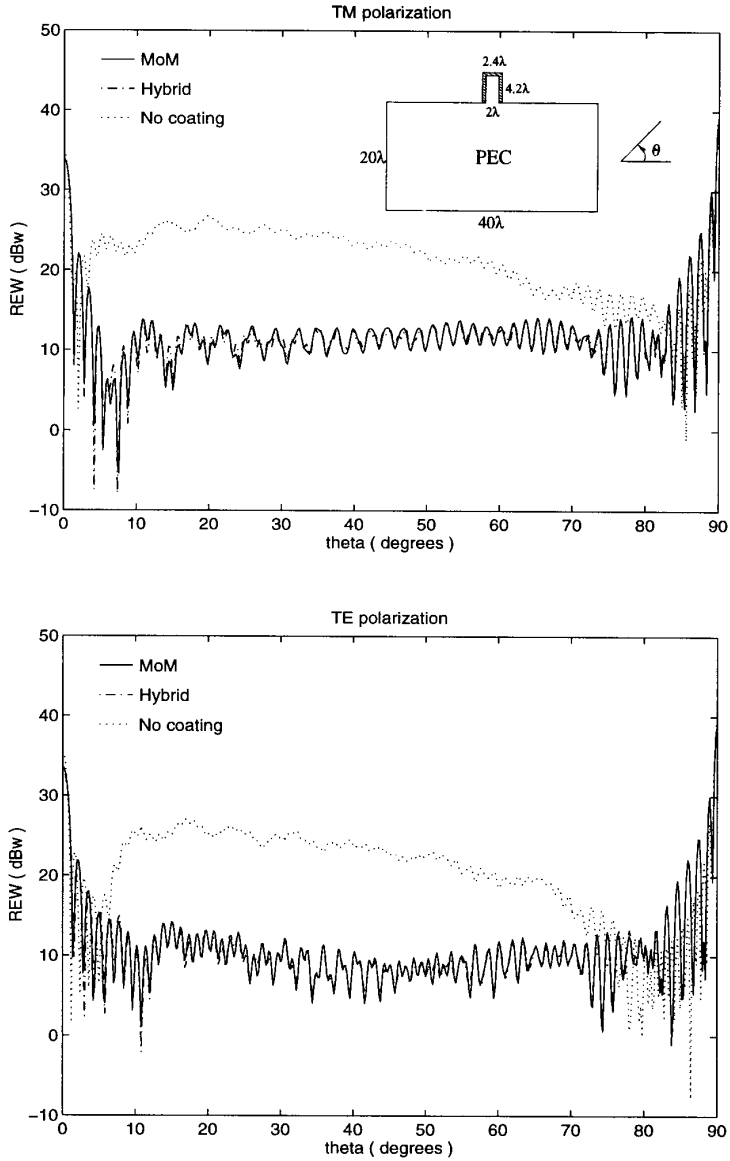

Figure 6. Comparison of the monostatic echo-width calculated by the hybrid SBR/MoM and the MoM for a body with a coated protrusion.

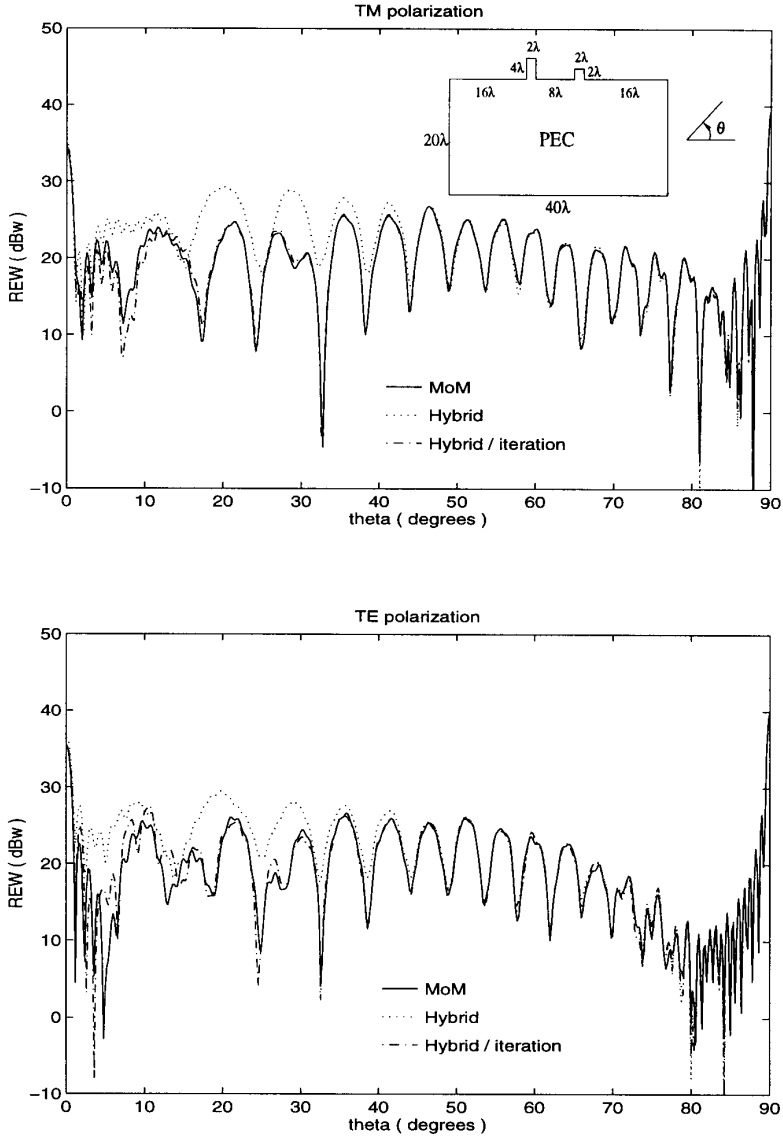

Figure 7. Comparison of the monostatic echo-width calculated by the hybrid SBR/MoM and the MoM for a body with two protrusions.

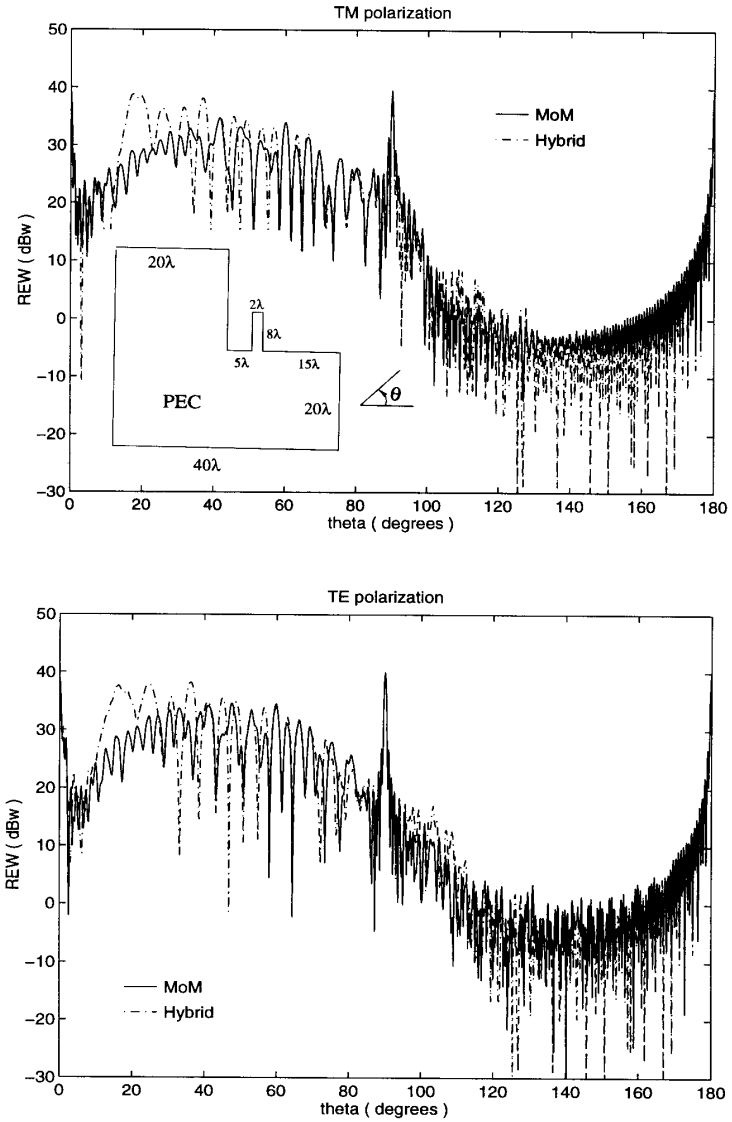

Figure 8. Comparison of the monostatic echo-width calculated by the hybrid SBR/MoM and the MoM for an L-shaped body with a protrusion.

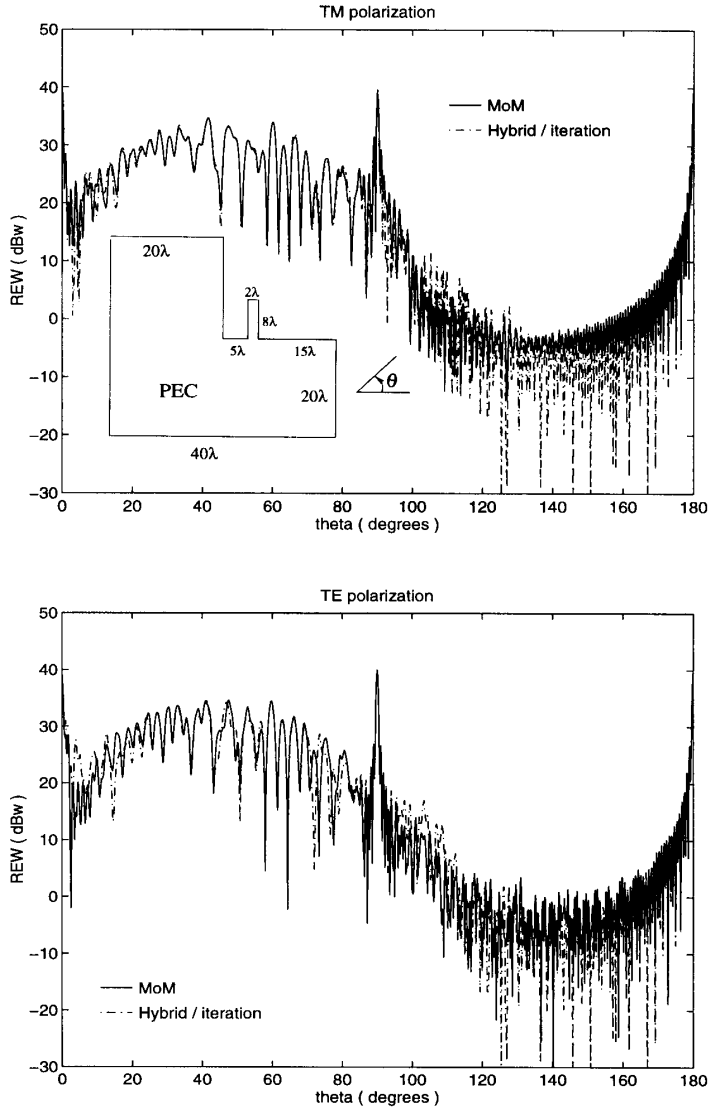

Figure 9. Comparison of the monostatic echo-width calculated by the hybrid SBR/MoM in conjunction with the iterative approach and the MoM for an L-shaped body with a protrusion.

360 unknowns and takes 16.1 seconds without iteration (Fig. 8) and 183.4 seconds with 10 iterations (Fig. 9).

4. CONCLUSION

A hybrid technique was presented for scattering by large bodies having small protruding structures. The technique combined the SBR method with the MoM in such a manner that the SBR and MoM computations could be carried out separately and yet all significant interactions were included. The technique calculated the scattered fields with the aid of the reciprocity theorem, which eliminated the need to resort to a complicated, time-consuming tracing of diverging rays. For problems which require higher accuracy than the hybrid solution would give, an iterative approach was designed to systematically improve the accuracy. The accuracy, efficiency, and capability of the hybrid technique were demonstrated using two-dimensional scattering examples. The technique is currently being extended to more challenging three-dimensional scattering problems.

ACKNOWLEDGEMENT

This work was supported by a grant from AFOSR via the MURI Program under contract number F49620-96-1-0025, the National Science Foundation under grant NSF ECE 94-57735, and the Office of Naval Research under grant N00014-95-1-0848. The authors wish to thank A. Greenwood for his helpful suggestions.

REFERENCES

1. Thiele, G. A., and T. H. Newhouse, "A hybrid technique for combining moment methods with the geometrical theory of diffraction," *IEEE Trans. Antennas Propagat.*, Vol. 23, 62–69, Jan. 1975.
2. Ekelman, E. P., and G. A. Thiele, "A hybrid technique for combining moment method treatment of wire antennas with the GTD for the curved surfaces," *IEEE Trans. Antennas Propagat.*, Vol. 28, 813–839, Nov. 1980.
3. Henderson, L. W., and G. A. Thiele, "A hybrid MM-GTD technique for treatment of wire antennas near a curved surfaces," *Radio Sci.*, Vol. 16, 1125–1130, 1981; Also, related paper in *IEEE Trans. Antennas Propagat.*, Vol. 30, 1257–1261, Apr. 1982.

4. Hsu, M., and P. H. Pathak, "Hybrid analysis (MM-UTD) of EM scattering from finned convex objects," *1995 IEEE AP-S Int. Symp. Dig.*, Vol. 3, 1456–1459, June 1995.
5. Jin, J. M., S. S. Ni, and S. W. Lee, "Hybridization of SBR and FEM for scattering by large bodies with cracks and cavities," *IEEE Trans. Antennas Propagat.*, Vol. 43, 1130–1139, Oct. 1995.
6. Greenwood, A. D., S. S. Ni, J. M. Jin, and S. W. Lee, "Hybrid FEM/SBR method to compute the radiation pattern from a microstrip patch antenna in a complex geometry," *Microwave Opt. Technol. Lett.*, Vol. 13, 84–87, Oct. 1996.
7. Wang, D. S., "Current-based hybrid analysis for surface-wave effects on large scatterers," *IEEE Trans. Antennas Propagat.*, Vol. 39, 839–849, June 1991.
8. Jakobus, U., and F. M. Landstorfer, "Improved PO-MM hybrid formulation for scattering from three-dimensional perfectly conducting bodies of arbitrary shape," *IEEE Trans. Antennas Propagat.*, Vol. 43, 162–169, Feb. 1995.
9. Obelleiro-Basteiro, F., J. L. Rodriguez, and R. J. Burkholder, "An iterative physical optics approach for analyzing the electromagnetic scattering by large open-ended cavities," *IEEE Trans. Antennas Propagat.*, Vol. 43, 356–361, Apr. 1995.
10. Jin, J. M., V. V. Liepa, and C. T. Tai, "A volume-surface integral equation for electromagnetic scattering by inhomogeneous cylinder," *J. Electromagn. Waves Appl.*, Vol. 2, No. 5/6, 573–588, 1988.
11. Jin, J. M., and V. V. Liepa, "Simple moment method program for computing scattering from complex cylindrical obstacles," *Proc. Inst. Elec. Eng.,* part H, Vol. 136, No. 4, 321–329, Aug. 1989.
12. Ling, H., R. C. Chou, and S. W. Lee, "Rays versus modes: Pictorial display of energy flow in an open-ended waveguide," *IEEE Trans. Antennas Propagat.,* Vol. AP-35, 605–607, May 1987.
13. Ling, H., R. C. Chou, and S. W. Lee, "Shooting and bouncing rays: calculating the RCS of an arbitrary shaped cavity," *IEEE Trans. Antennas Propagat.,* Vol. AP-37, 194–205, Feb. 1989.
14. Baldauf, J., S. W. Lee, L. Lin, S. K. Jeng, S. M. Scarborough, and C. L. Yu, "High frequency scattering from trihedral corner reflectors and other benchmark targets: SBR vs. experiments," *IEEE Trans. Antennas Propagat.,* Vol. AP-39, 1345–1351, Sept. 1991.